Journal of Cancer Research and Clinical Oncology
https://doi.org/10.1007/s00432-022-04253-1

RESEARCH

Heterogeneous expression of ACE2, TMPRSS2, and FURIN at single-cell resolution in advanced non-small cell lung cancer

Zeyu Liu[1] · Xiaohua Gu[1] · Zhanxia Li[1] · Shan Shan[1] · Fengying Wu[2] · Tao Ren[1]

Received: 16 April 2022 / Accepted: 2 August 2022

Abstract

Purpose Considering the high susceptibility of patients with advanced non-small cell lung cancer (NSCLC) to COVID-19, we explored the susceptible cell types and potential routes of SARS-CoV-2 infection in lung adenocarcinoma (LUAD) and lung squamous cell carcinoma (LUSC) by analyzing the expression patterns of the entry receptor angiotensin converting enzyme 2 (*ACE2*) and the spike (S) protein priming proteases transmembrane serine protease 2 (*TMPRSS2*) and *FURIN*.

Methods Single-cell transcriptomic analysis of 14 LUSC and 12 LUAD samples was utilized to exhibit the heterogeneous expression of *ACE2*, *TMPRSS2* and *FURIN* across different cell subsets and individuals.

Results 12 cell types and 33 cell clusters were identified from 26 cancer samples. *ACE2*, *TMPRSS2* and *FURIN* were heterogeneously expressed across different patients. Among all cell types, *ACE2*, *TMPRSS2* and *FURIN* were predominately expressed in cancer cells and alveolar cells, and lowly uncovered in other cells. Compared to LUSC, the protein priming proteases (*TMPRSS2* and *FURIN*) were highly found in LUAD samples. However, *ACE2* was not differentially expressed in cancer cells between the two cancer types. Moreover, *ACE2*, *TMPRSS2*, and *FURIN* expressions were not higher in any cell type of smokers than non-smokers.

Conclusion Our research first revealed the heterogeneous expression of *ACE2*, *TMPRSS2*, and *FURIN* in different cell subsets of NSCLC and also across different individuals. These results provide insight into the specific cells targeted by SARS-CoV-2 (i.e., cancer cells and alveolar cells) in patients with advanced NSCLC, and indicate that smoking may be not an independent risk factor for NSCLC combined with COVID-19.

Keywords *ACE2* · *TMPRSS2* · *FURIN* · Non-small cell lung cancer · Tumor heterogeneity

Introduction

Coronavirus disease 2019 (COVID-19) is an acute respiratory infection triggered by SARS-CoV-2, which has created a global pandemic (Jackson et al. 2022). To date (December 29, 2021), COVID-19 has resulted in 281,808,270 laboratory-confirmed human infections globally and has accounted for more than 5411 thousand deaths, as reported by the WHO. SARS-CoV-2 infects individuals via its S protein, which binds to the *ACE2* receptor, followed by priming through two host cell enzymes, the TMPRSS2 and the protease FURIN (Hoffmann et al. 2020a, 2020b). Contributing to SARS-CoV-2 host cell entry, ACE2 and its co-factors TMPRSS2 and FURIN show a significant correlation with host cell susceptibility in SARS-CoV-2 infection.

Lung cancer is also common globally at a high incidence and mortality rate (Yang et al. 2020), in which NSCLC accounts for 85–90% of cases (Chang et al. 2015). Patients

Zeyu Liu and Xiaohua Gu contributed equally to this work.

✉ Shan Shan
shanshan_shcn@126.com

✉ Fengying Wu
fywu@163.com

✉ Tao Ren
liuyuanrentao@sjtu.edu.cn

[1] Department of Respiratory and Clinical Care Medicine, Shanghai Jiao Tong University Affiliated Sixth People's Hospital, Shanghai 200233, China

[2] Department of Medical Oncology, Shanghai Pulmonary Hospital, Tongji University School of Medicine, Shanghai 200433, China

Published online: 12 August 2022

with lung carcinoma, especially NSCLC, have a higher vulnerability to SARS-CoV-2 and higher rates of serious complications, leading to the admission to intensive care unit or even death than normal persons (Onder et al. 2020; Rogado et al. 2020; Zhou et al. 2020). This could potentially be attributed to the systemic immunosuppressive state induced by the malignancy or anti-tumor treatments (Addeo et al. 2020). However, it has also been shown that irrespective of active anticancer treatments, patients with cancer still have an excess risk of suffering from COVID-19 (OR, 2.31; 95% CI, 1.89–3.02), relative to the general population (Yu et al. 2020). We, therefore, infer that other mechanisms contribute to the high susceptibility of patients with NSCLC to SARS-CoV-2, such as the heterogeneous expressions of ACE2, TMPRSS2 and FURIN across cell subsets and individuals.

LUSC and LUAD account for about 80% of NSCLC cases (Herbst et al. 2008). According to some bioinformatics assays, *ACE2* mRNA expression is upregulated in LUAD (Chai et al. 2020; Kong et al. 2020). In LUSC, ACE2 expression levels are similar to those in normal lung tissues, except in the primitive subtype (Kong et al. 2020). Additionally, *TMPRSS2* expression levels are lower in LUAD and LUSC than those in healthy lung tissues (Kong et al. 2020). However, these genes' expression patterns across different cell types and individuals are still unclear. In our research, single-cell RNA sequencing (scRNA-seq) of 26 biopsy samples, including 14 LUSC samples and 12 LUAD samples, were acted to explore the expression levels of *ACE2*, *TMPRSS2*, and *FURIN* in cancer cells and the tumor microenvironment (TME), which consists of stromal cells, infiltrating immune cells, alveolar cells and other cell types (Chen et al. 2015). Of note, our data revealed vast tumoral heterogeneity among cancer and TME cells in different patients. Our study provides the first evidence for the heterogeneous expression of *ACE2*, *TMPRSS2*, and *FURIN* across different cell subsets of LUSC and LUAD tissue samples and provides insight into the intrinsic factors correlated with COVID-19 infection in NSCLC patients.

Materials and methods

Patients

All patients were histologically diagnosed as advanced NSCLC and further classified as smokers (not less than 20 packs/year and quitting less than 10 years prior to enrollment) and non-smokers (less than 100 cigarettes during the lifetimes). From November 2018 to August 2019, the tissue samples were obtained from the primary lung tumor by bronchoscopy or transcutaneous needle biopsy. Patient information is available in (Table 1). This research was supported by the Ethical Committee of Shanghai Pulmonary Hospital (K18-089-1).

Tissue dissociation and preparation of single-cell suspensions

Total specimens were used for scRNA-seq. Fresh biopsy samples were rinsed in Hanks Balanced Salt Solution and then sliced to less than 1 mm pieces. The tissue pieces were digested with dissociation buffer for 10 to 20 min at 37 °C with continuous gentle rocking. Following digestion, single cells were separated from cell debris and other impurities using a sterile strainer (40-micron; Corning, Inc., Corning, NY, USA). Dissociated cells were incubated with Red Blood Cell Lysis Buffer (Singleron Biotechnologies, Nanjing, China) for 10 min at 25 °C and then washed thoroughly in PBS (HyClone, Logan, UT, USA) to gain a single-cell suspension. The final suspension was centrifuged and resuspended in PBS at a density of 1×10^5 cells/ml.

Single-cell RNA sequencing library preparation

The final single-cell suspension was loaded onto a microfluidic chip to generate the scRNA-seq libraries according to the manufacturer's instructions (GEXSCOPE Single-Cell RNA-seq Kit, Singleron Biotechnologies). The resulting libraries were sequenced using an Illumina Hi-Seq × 10 platform to obtain 150 bp paired-end reads.

All the tissue preparation, sequencing and further data analysis works were done by Singleron Biotechnologies Ltd. (Nanjing, China). The laboratories, experimental protocols or sequencing platform were highly consistent across different samples.

Quality control, cell type clustering and major cell type identification

Gene expression matrices were generated from raw reads using scopetools (https://anaconda.org/singleronbio/scopetools). Cells with < 200 or > 5,000 expressed genes, or more than 30,000 unique molecular identifiers (UMIs), or mitochondrial contents exceeding 30% were removed. After doublet removal, we obtained 78,766 cells for further analysis. The average number of genes and UMIs for each sample is shown in Table S1. We selected the top 600 variable genes using the Seurat 2.3 FindVariable function and then a principal component analysis was applied. The top 20 principal components, a resolution of 1.0 and the FindClusters function were used to generate 33 cell clusters. Each cluster was scored according to the normalized expression levels of canonical markers and assigned to the cell type with the highest score. Clusters belonged to the same cell type were grouped for the next analysis. The results were confirmed

Table 1 Demographics and clinical characteristics of study subjects

Patient number	Gender	Age year	Cancer types	Biopsy site	Smoking status	Stage
P3	Male	67	LUSC	Lung	Y	IV
P41	Male	60	LUSC	Lung	Y	IV
P1	Female	71	LUSC	Lung	N	IV
P7	Male	71	LUSC	Lung	Y	IV
P15	Male	64	LUSC	Lung	N	IV
P18	Male	66	LUSC	Lung	N	IV
P23	Male	77	LUSC	Lung	Y	IV
P4	Male	58	LUSC	Lung	Y	IIIc
P17	Male	71	LUSC	Lung	Y	IIIb
P10	Male	65	LUSC	Lung	Y	IIIb
P25	Male	75	LUSC	Lung	Y	IIIb
P14	Male	60	LUSC	Lung	Y	IIIc
P40	Male	62	LUSC	Lung	Y	IIIc
P29	Male	48	LUAD	Lung	Y	IV
P8	Male	35	LUAD	Lung	N	IV
P39	Male	49	LUAD	Lung	N	IV
P12	Female	62	LUAD	Lung	N	IV
P38	Male	55	LUAD	Lung	Y	IV
P28	Female	64	LUAD	Lung	N	IV
P35	Male	63	LUAD	Lung	Y	IV
P13	Female	50	LUAD	Lung	N	IV
P21	Male	65	LUAD	Lung	Y	IV
P5	Male	62	LUAD	Lung	N	IV
P16	Male	49	LUAD	Lung	Y	IV
P6	Male	59	LUSC	Lung	N	IV
P9	Male	40	LUAD	Lung	Y	IIIc

to be correct by manual inspection and were visualized through uniform manifold approximation and projection (UMAP). Twelve cell subtypes were determined by an initial exploratory inspection of the differentially expressed genes in each cluster corresponded to the reported cell-type specific marker genes. The differentially expressed genes were generated using the Seurat FindMarkers function. scRNA-Seq data were uploaded to NCBI Gene Expression Omnibus database (GSE148071).

LUAD and LUSC classification based on scRNA-seq expression

LUAD and LUSC scores were identified relied on the average percentage of tumor cells with marker expression for LUAD (NAPSA and TTF-1) or LUSC (KRT5 and TP63) (Fig. S1). Each patient was assigned to the subtype with the highest score. A final classification was determined by experts according to an integrated consideration of pathological subtype and scRNA-seq subtype assignments. Group determination in all subsequent analyses was relied on the final patients' classification.

ACE2, *FURIN* and *TMPRSS2* expression based on scRNA-seq data

The distributions of *ACE2*, *FURIN*, and *TMPRSS2* expression across distinct patients and cell types were evaluated based on scRNA-seq data. Gene expression patterns of *ACE2*, *TMPRSS2* and *FURIN* were visualized by UMAP plots, box plots, and bubble plots.

Statistical analysis

All values were expressed as means ± SD. Differences were assessed by the Wilcoxon rank-sum test, and $P < 0.05$ was considered statistically significant.

Results

Establishment of a cell atlas

scRNA-seq data for 26 advanced NSCLC patient samples with various histological and molecular phenotypes were

analyzed (Fig. 1A, Table 1). After multiple quality control and filtering steps, transcriptome data for 78,766 cells were analyzed and then divided into 33 clusters by unsupervised clustering, as shown on UMAP plot (Fig. 1B). Nine major cell types, including cancer cells, alveolar cells, fibroblasts, endothelial cells, epithelial cells other than carcinoma cells, lymphocytes, plasma cells, myeloid cells and mast cells, were further confirmed and assigned to each cluster based on the expression of canonical cell markers (Fig. 1B–D). The relative frequencies of different cell types varied substantially among specimens, which could be attributed to locations within the tumor or different tumor phenotypes (Fig. 1E). For deeper insight and more precise assessment, we further subdivided immune cells into seven cell types, which includes plasma cells, mononuclear phagocytes (MP), *T* cells, mast cells, *B* cells, neutrophils and mature DC (Fig. S2). The numbers for each cell type are listed in Table S2. For better visualization, a stacked bar plot of non-cancer cells was displayed in Fig. S3.

We next evaluated the intertumoral heterogeneity across patients. One may observe that clusters defined as cancer cells are mainly contributed by sole individual patients while the remaining clusters defined as immune cells, stromal cells or alveolar cells are shared by multiple patients (Fig. 1A–C). According to these clustering results, cancer cells of different patients showed an enhanced heterogeneity and patient-specific expression phenotypes compared to stromal and immune cells, which clustered together across different patients. In addition, we also used principal component analysis (PCA)-based method to measure the intertumoral heterogeneity levels of cancer cells according to the procedure reported in the literature (Zhang et al. 2021). The global or patient average in the principal component (PC) space were calculated by averaging the PC scores for all cancer cells or cancer cells from each patient. The inter-tumoral heterogeneity is characterized by the distance of patient average in each sample and global average (Fig. S4).

Heterogeneous expression of *ACE2*, *FURIN* and *TMPRSS2* across cell subtypes and individuals

We detected significant differences in the expression levels of *ACE2*, *FURIN*, and *TMPRSS2* across cell subtypes (Fig. 2A, B) and individuals (Fig. 2C). Heterogeneity in gene expression is common among individuals with advanced NSCLC. Frequencies of *ACE2*, *FURIN*, *and TMPRSS2*-positive cells from each cell subtypes per patient are shown in Table S3.

Comparison of *ACE2*, *FURIN*, and *TMPRSS2* expression across different cell subsets between LUAD and LUSC

A total of 26 patients included 12 (46.2%) LUAD and 14 (53.8%) LUSC. Based on morphology and function, twelve total cell subtypes were classified into five major cell types, including cancer cell types, immune cell types (*T* cells, *B* cells, plasma cells, MP, neutrophils, mature DC, and mast cells), alveolar cells, epithelial cells other than cancer cells, and stromal cell types (fibroblasts and endothelial cells). According to the contents in biopsy samples and the proportion of positive cells in each cell type, we focused on three of the five major cell types, including cancer cells, immune cells (MP, plasma cells, *T* cells, and mast cells), and alveolar cells. The levels and frequencies of *ACE2*, *FURIN*, and *TMPRSS2* expression in cell types mentioned above were analyzed in LUAD and LUSC.

We first examined the levels and frequencies of *ACE2*, *FURIN*, and *TMPRSS2* expression in cancer cells between LUAD and LUSC (Fig. 3A, B). We detected a higher level and frequency of *TMPRSS2* expression in LUAD cancer cells than in LUSC cancer cells ($P < 0.01$), while *ACE2* and *FURIN* showed no significant differences (Fig. 3B).

According to the characteristic markers ABCA3, alveolar cells were identified and compared among cancer types (Fig. 3C,D). The levels and proportions of cells expressing *ACE2, FURIN* and *TMPRSS2* in alveolar cells of LUAD patients were higher than those in LUSC patients , while *FURIN and TMPRSS2* showed higher levels of significance ($P < 0.01$) (Fig. 3D). Of note, alveolar cells were only detected in eleven samples, and nine samples were obtained from patients with LUAD; accordingly, additional data are needed to verify these findings.

All immune cells in the two cancer types were divided into seven cell subtypes, and MP, plasma cells, *T* cells, as well as mast cells are the major components (Fig. 4A). We found that *ACE2*, encoding the entry receptor of S protein, and *TMPRSS2* were rarely expressed in immune cells (Fig. 2B). *FURIN* expression was detected in immune cells (MP, plasma cells, *T* cells, and mast cells) (Fig. 4B), and had no significant difference between LUAD and LUSC (Fig. 4C).

The exact number and percentage of *ACE2*, *FURIN*, *and TMPRSS2*-positive cells of the total cells in each cell type between LUAD and LUSC are shown in Table S4. Furthermore, we also perform batch correction in Harmony prior to clustering analysis and compare the results and conclusions to the existing analysis. The latter conclusions when looking at levels and frequencies of *ACE2*, *FURIN*, and *TMPRSS2* expression across donor groups were consistent with the previous findings, and the UMAP visualization of these genes after removal of the batch effect is displayed in Fig. S5.

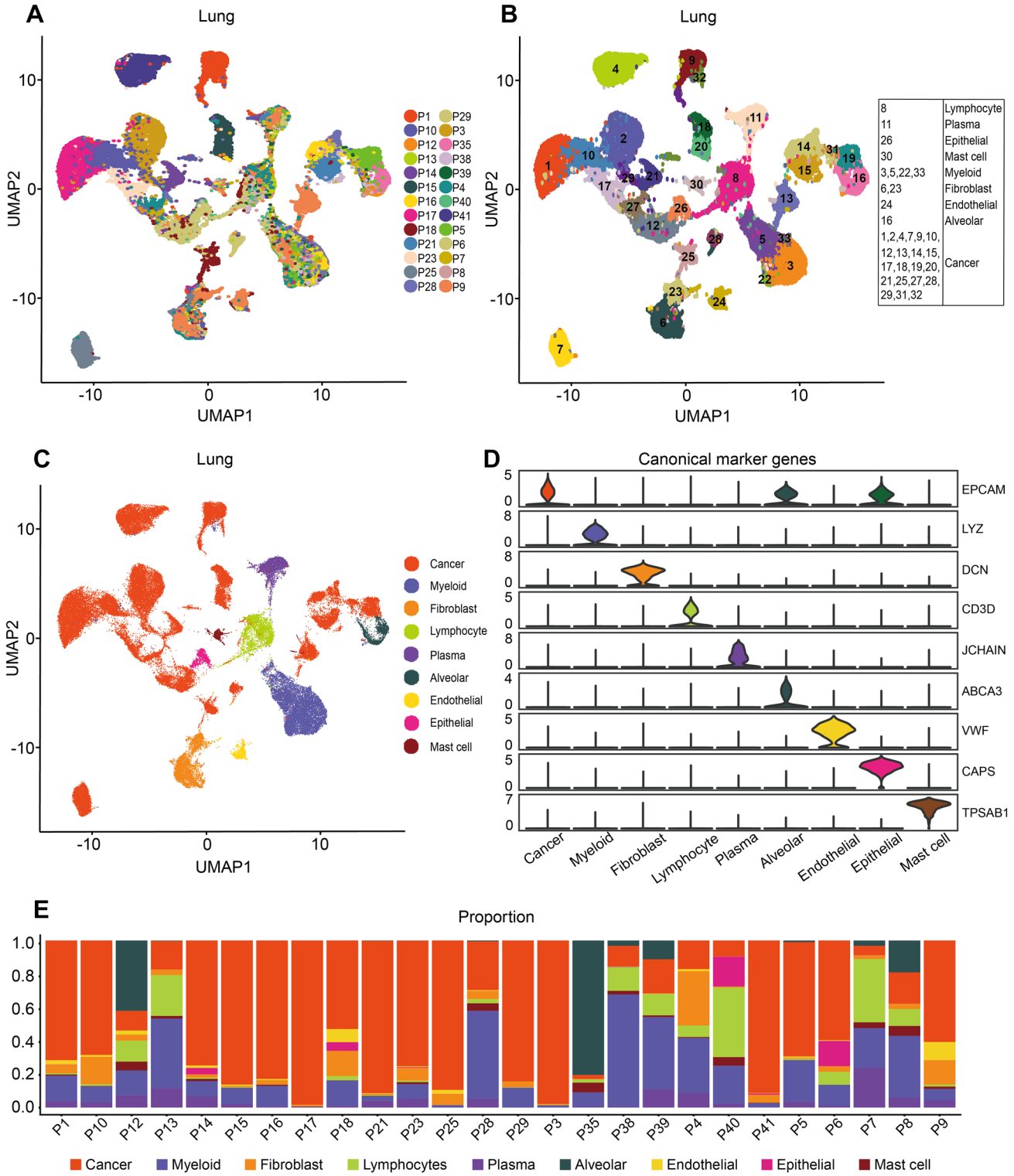

Fig. 1 Heterogeneity and patient-specific expression signatures determined from biopsy samples. **A** UMAP analysis of 78,766 cells from 26 patients with NSCLC. **B**, **C** UMAP clustering of all cells. In total, 33 cell clusters and 9 major cell types were identified across 78,766 cells. **D** Violin plots showing expression of canonical cell-type marker genes across 9 major cell types. Cancer cell types were positive for EPCAM while negative for epithelial marker CAPS and alveolar marker ABCA3. **E** The distributions of major cell types varied among samples

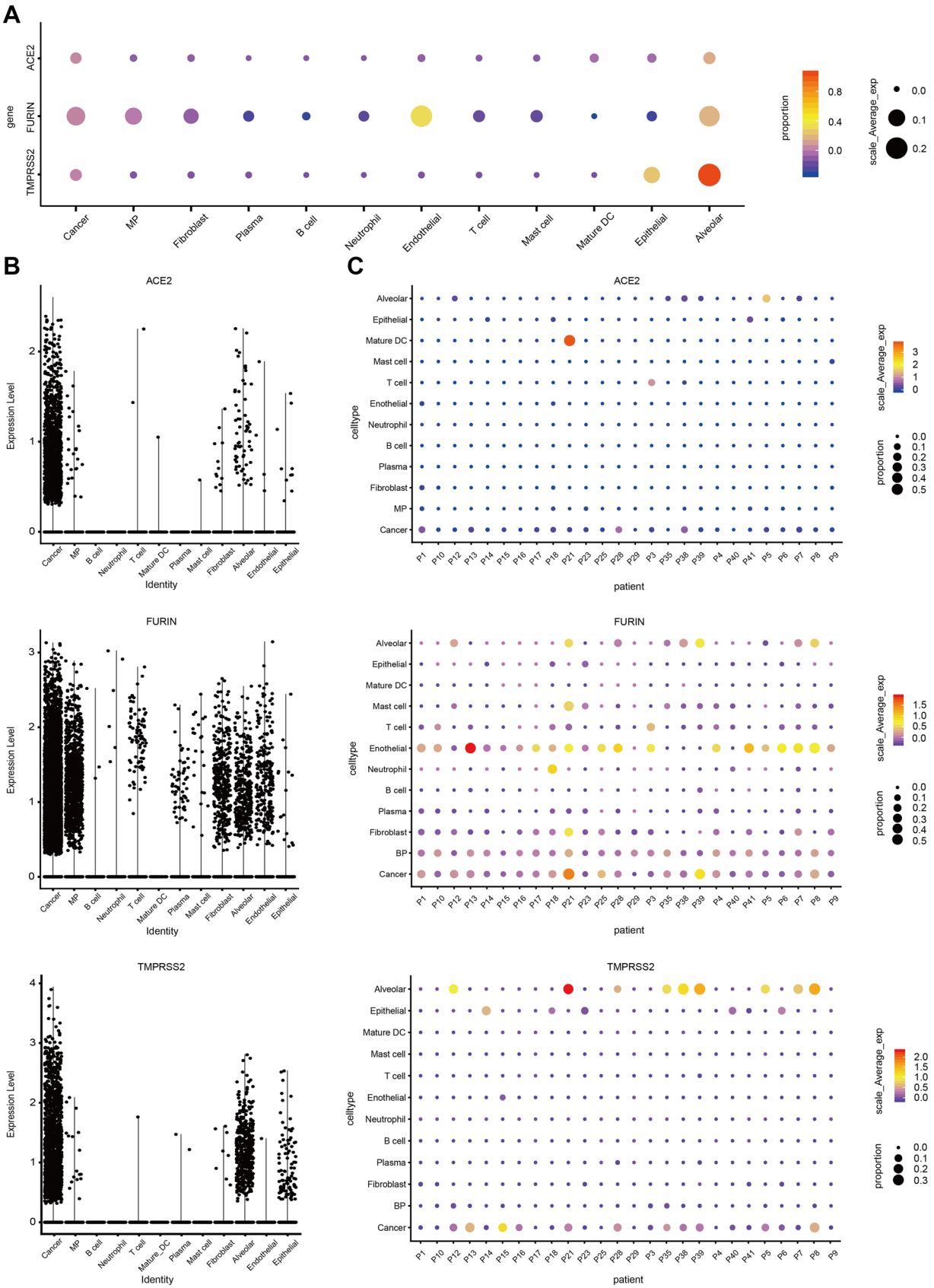
A
gene
ACE2
FURIN
TMPRSS2
Cancer
MP
Fibroblast
Plasma
B cell
Neutrophil
Endothelial
T cell
Mast cell
Mature DC
Epithelial
Alveolar
proportion
0.8
0.4
0.0
scale_Average_exp
0.0
0.1
0.2
B
ACE2
Expression Level
Identity
C
ACE2
celltype
patient
scale_Average_exp
proportion
FURIN
TMPRSS2
BP

◂**Fig. 2** Proportion and average expression of *ACE2, FURIN*, and *TMPRSS2* across cell subsets and individuals. **A** Dot plot of the proportion of cells (dot size) in each cell subtype expressing *ACE2, FURIN*, and *TMPRSS2* and average expression (color scale). **B** Point plots of the *ACE2*, *FURIN*, and *TMPRSS2* expression levels in each cell subtype. **C** Dot plot of the proportion of cells (dot size) from each patient expressing *ACE2*, *FURIN* and *TMPRSS2* and average expression (color scale)

Comparison of *ACE2*, *FURIN*, and *TMPRSS2* expression across different cell subsets between non-smoking and smoking groups

26 patients were divided into smokers and non-smokers according to their smoking habits. The average expression levels and proportion of cells expressing *ACE2*, *FURIN*, and *TMPRSS2* in the cell type mentioned above were analyzed next.

The levels and proportions of cancer cells expressing *ACE2* and *TMPRSS2* were slightly raised in non-smokers; however, the levels and frequencies of *FURIN* expression did not differ significantly with respect to smoking status (Fig. 5A).

Moreover, *ACE2*, *FURIN*, and *TMPRSS2* expression levels in alveolar cells (Fig. 5B), and *FURIN* expression levels in immune cells (MP, plasma cells, *T* cells, and mast cells) showed no statistical difference between the smoking and non-smoking groups (Fig. 5C). These findings were consistent with some research which indicated that smoking was not an independent epidemiological risk factor for COVID-19 (Rossato et al. 2020; Williamson et al. 2020).

The exact number and percentage of *ACE2*, *FURIN*, *and TMPRSS2*-positive cells of the total cells in each cell type between smoking and non-smoking groups are shown in Table S5.

Discussion

In this research, we obtained a comprehensive landscape of cell types in LUSC and LUAD from 26 biopsy samples by scRNA-seq. TME cells of different patients, including immune cells, stromal cells, epithelial cells, and alveolar cells clustered together by cell type, while cancer cells exhibited relatively high heterogeneity and patient-specific expression profiles. Lung cancer is a heterogeneous disease, and its heterogeneity has implications for diagnosis, selection of tissues for molecular diagnosis, therapeutic decisions as well as disease processes at the cellular and histological levels (Sousa, Carvalho. 2018). In our study, we further identified inter-tumoral heterogeneity of lung cancer at a cellular and molecular level. The heterogeneous expression patterns of *ACE2*, *TMPRSS2*, *and FURIN* among cell subsets from LUSC and LUAD tissue samples and among individuals were revealed for the first time. We inferred that tumor molecular heterogeneity can explain, in part, why patients with NSCLC show significant differences in susceptibility to SARS-CoV-2 and illness severity.

LUSC and LUAD, as two major pathological subtypes of NSCLC, differ in origin, biological patterns and molecular characteristics (Xu et al. 2018). Recently, some studies have reported that susceptibility to SARS-CoV-2 might be higher in LUAD than in LUSC (Kong et al. 2020). The main mechanism underlying the interaction between SARS-CoV-2 and mammalian host cells is the binding of the S protein of SARS-CoV-2 to its receptor human ACE2 (hACE2) through its receptor-binding domain and proteolytic pre-activation by TMPRSS2 and FURIN (Shang et al. 2020). Detailed analyses of the differences in *ACE2*, *TMPRSS2*, *and FURIN* expression levels between LUAD and LUSC may clarify whether cancer itself alters SARS-CoV-2 susceptibility phenotypes and disease severity.

Therefore, we explored the RNA expression levels of *ACE2*, *TMPRSS2*, *and FURIN* in 26 biopsy samples, including 14 LUSC samples and 12 LUAD samples. Cancer cells were the major cells in each biopsy sample, with the highest frequencies of all detected cell types. Our data inferred that *ACE2, TMPRSS2*, and *FURIN* were all expressed in cancer cells. Cancer cells expressing *TMPRSS2* in LUAD was more than that in LUSC, while *FURIN* and *ACE2* expression did not differ between two cancer types. These results were consistent with those of bioinformatics studies (Chai et al. 2020; Kong et al. 2020). Hence, LUAD patients were probably at a greater infectious risk of SARS-CoV-2.

TME, composed of diverse cell types (epithelial cells, alveolar cells, immune cells, stromal cells, etc.) and extracellular components, surrounds cancer cells and influences tumor initiation, progression, metastasis, as well as therapeutic efficacy (Binnewies et al. 2018; Ostman. 2012, Wu, Dai 2017). ACE2 and its cofactor TMPRSS2 are highly expressed on type 2 alveolar cells, which may act as target cells in humans (Zou et al. 2020). Our data inferred that alveolar cells expressed *ACE2, TMPRSS2*, and *FURIN*. The average proportion of alveolar cells expressing *ACE2*, *FURIN* and *TMPRSS2* was higher in LUAD than in LUSC. As a result, alveolar cells in patients with LUAD may be more vulnerable to SARS-CoV-2. However, alveolar cells only existed in several samples in our study, and most samples were taken from patients with LUAD; more data are needed to support these findings. In addition, only *FURIN* was expressed in immune cells, which contains MP, plasma cells, T cells, and mast cells. It is possible that some types of immune cells in TME mentioned above are not target cells of SARS-CoV-2 and only participate in the progression of COVID-19 via the immune and inflammation response (Paces et al. 2020).

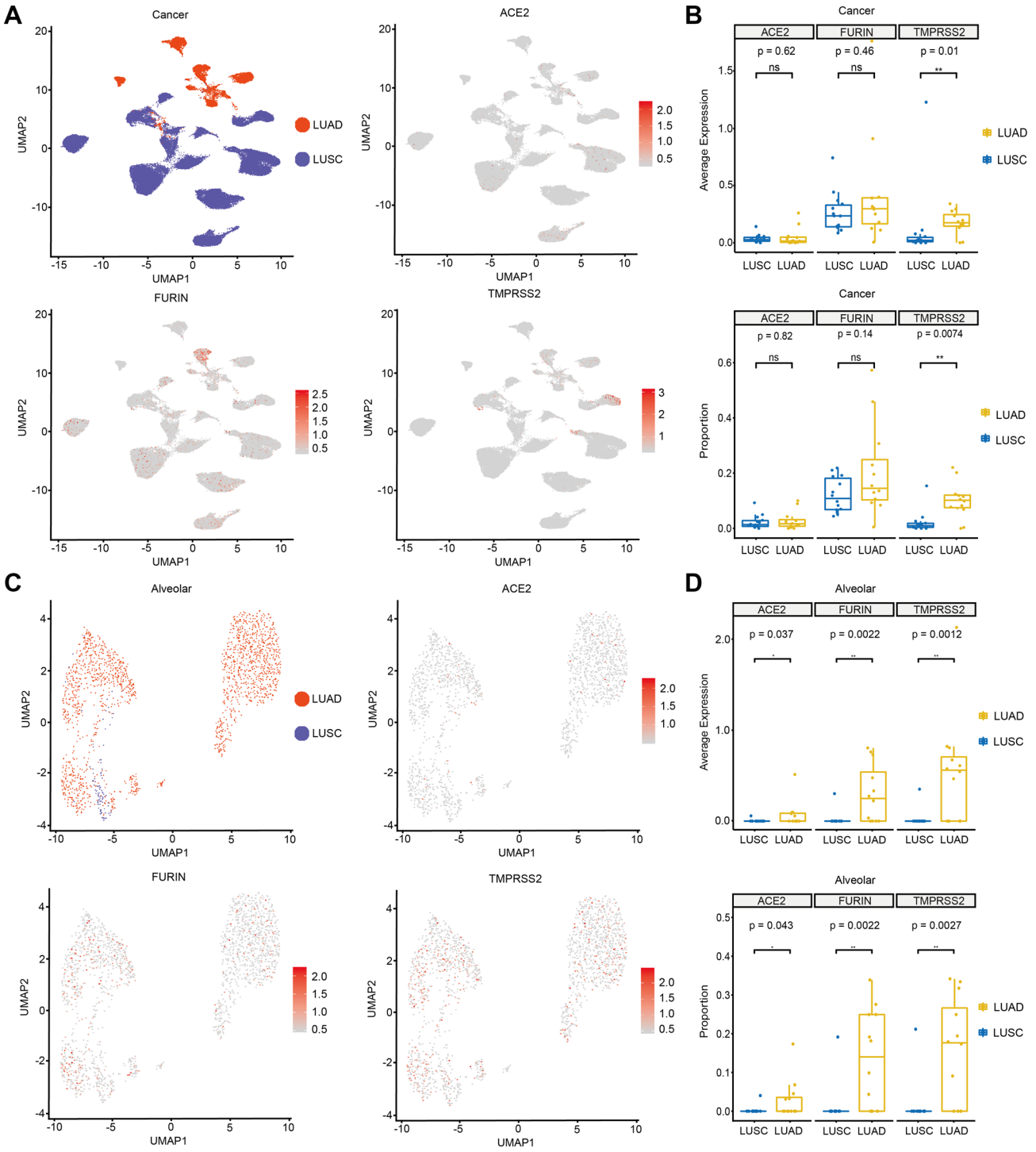

Fig. 3 *ACE2*, *FURIN*, and *TMPRSS2* expression patterns in cancer and alveolar cells between LUAD and LUSC. **A** Cancer cells were identified as LUAD and LUSC. *ACE2*, *FURIN*, and *TMPRSS2* expression patterns in cancer cells were detected and shown on UMAP plot. **B** Box plots of *ACE2, FURIN*, and *TMPRSS2* expression levels and proportions in cancer cells across LUAD and LUSC. **C** Alveolar cells were grouped as LUAD and LUSC according to donor group. *ACE2*, *FURIN*, and *TMPRSS2* expression patterns in all alveolar cells were detected. **D** Box plots of *ACE2, FURIN*, and *TMPRSS2* expression levels and proportions in all identified alveolar cells between LUAD and LUSC

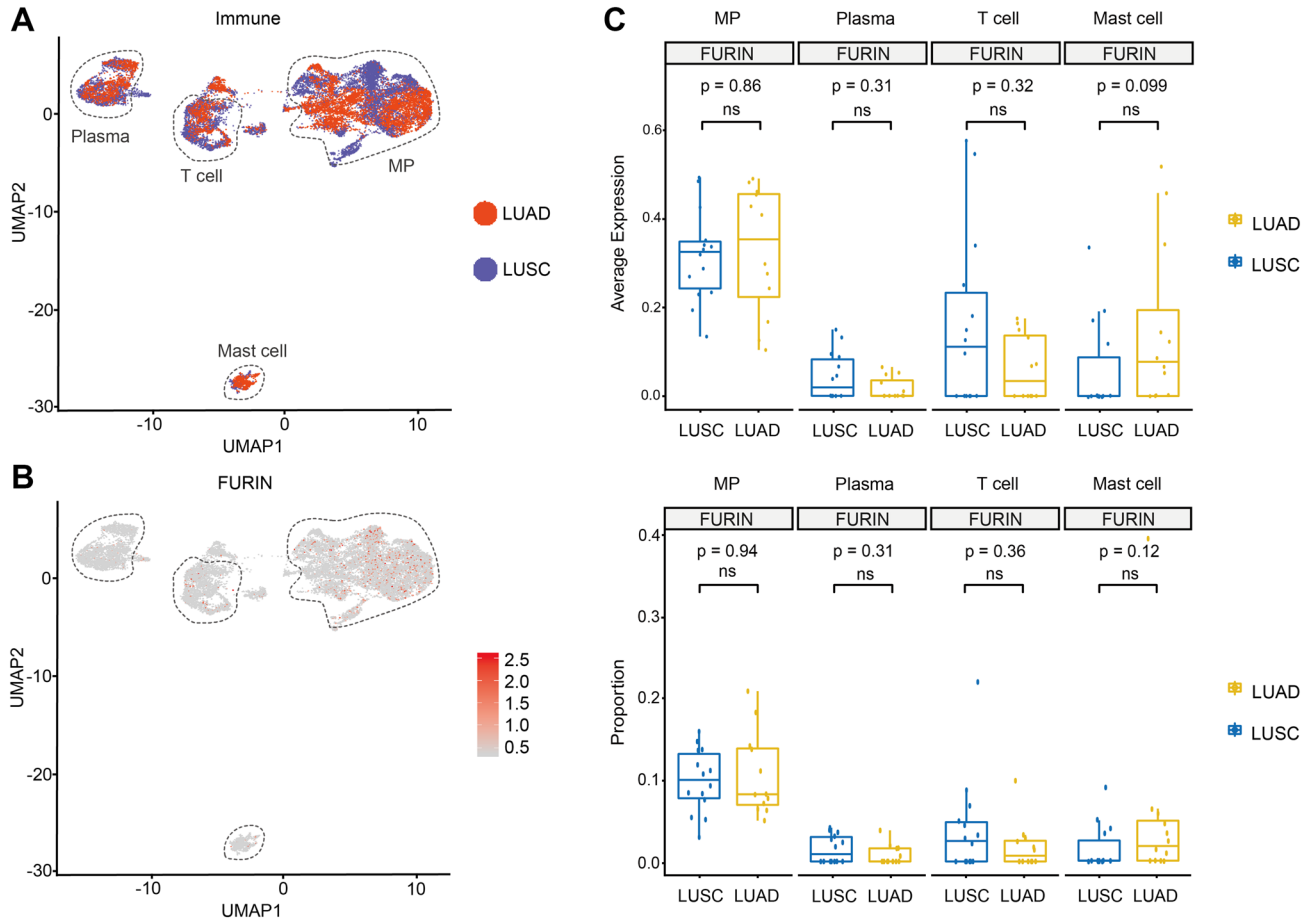

Fig. 4 *FURIN* expression patterns in immune cells between LUAD and LUSC. **A** Immune cells were grouped as LUAD and LUSC according to donor group, and could be divided into seven cell subtypes according to marker expression. MP, plasma cells, *T* cells, and mast cells are the major components. **B** *FURIN* expression patterns in all immune cells were detected. **C** Box plots of *FURIN* expression levels and proportions in MP, plasma cells, *T* cells, and mast cells between LUAD and LUSC

Smoking is an important risk factor for lung cancer and can influence the pulmonary TME (Giotopoulou, Stathopoulos 2020). A previous study has shown that smoking triggers an increase in ACE2 expression, which may partially predict that smokers possibly have an enhanced severe COV-19 susceptibility (Smith et al. 2020). However, in our datasets, we could not find that the average expression and frequencies of *ACE2*, *TMPRSS2*, and *FURIN* were higher in any cell type of smokers than non-smokers. These may indicate that smoking was not an independent risk factor for NSCLC combined with COVID-19. These findings were consistent with the conclusions of some clinical observations (Rossato et al. 2020).

In addition, we found that ACE2 expression levels in cancer cells between LUAD and LUSC were no significant differences, which brings new thinking to the susceptibility of variant of SARS-CoV-2 that mainly relied on binding to ACE2 but not depended on TMPRSS2 (Meng et al. 2022).

To sum up, our results provide insight into the molecular basis for the higher risk of SARS-CoV-2 infection and worse prognosis in LUAD patients compared to LUSC patients and show that disease progression in patients with lung cancer could not be aggravated by smoking. Cancer cells and alveolar cells in the TME might act as target cells. Remarkably, we provide the first evidence for the heterogeneous expression of *ACE2, TMPRSS2*, and *FURIN* across cell subsets and individuals in NSCLC, explaining the observed variation in susceptibility and severity of SARS-CoV-2 infection. Individualized prevention methods and treatments are necessary to meet the needs of different patients with NSCLC during the ongoing COVID-19 pandemic.

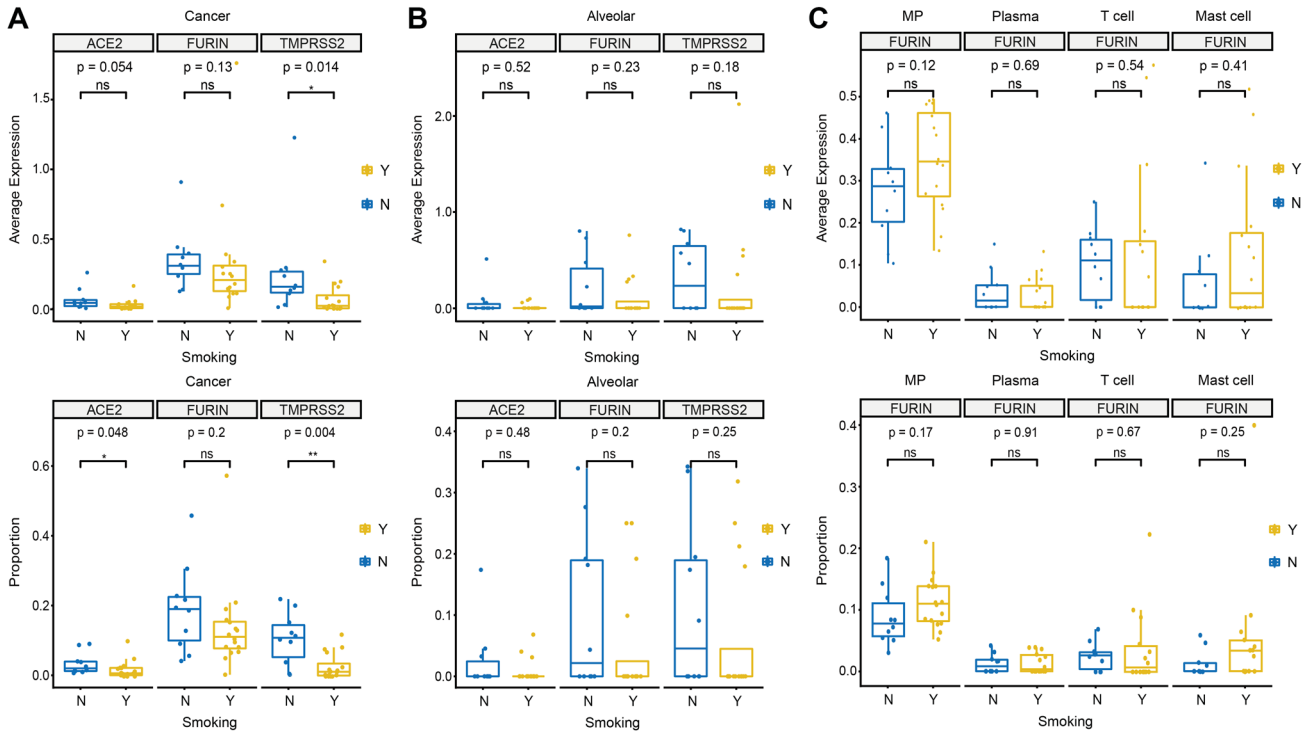

Fig. 5 *ACE2, FURIN*, and *TMPRSS2* expression patterns in major cell types between the smoking and non-smoking groups. **A**, **B** Box plots of *ACE2*, *FURIN*, and *TMPRSS2* expression levels and proportions in cancer cells **A** and alveolar cells **B** across the smoking and non-smoking groups. **C** Box plots of *FURIN* expression levels and proportions in MP, plasma cells, *T* cells, and mast cells between the smoking and non-smoking groups

Supplementary Information The online version contains supplementary material available at https://doi.org/10.1007/s00432-022-04253-1.

Acknowledgements We thank every patient who donated tissue samples in this study. We are grateful to Singleron Biotechnologies Ltd. (Nanjing, China), for technical assistance on sequencing assays. This research was approved by National Nature Science Foundation of China (81930001, 81902314, 81870055), Medical-Engineering Cross Project of Shanghai Jiao Tong University (YG2020YQ18), Clinical Research Plan of SHDC (No. SHDC2020CR4001), and Shanghai Nature Science Foundation (20ZR1447100).

Author contributions TR, FW and SS: were responsible for the conception and design of the study. ZL and XG: contributed to the data collection and analyses. ZL, XG, and ZL: wrote the manuscript, and revised as needed under the guidance of SS, TR and FW. All authors approved the final version.

Funding This work was supported by National Nature Science Foundation of China (81930001, 81902314, 81870055), Medical-Engineering Cross Project of Shanghai Jiao Tong University (YG2020YQ18), Clinical Research Plan of SHDC (No. SHDC2020CR4001), and Shanghai Nature Science Foundation (20ZR1447100).

Data availability The datasets in this study can be found online, https://www.ncbi.nlm.nih.gov/, GSE148071.

Declarations

Competing interests The authors declare no competing interests.

Conflict of interest The authors commit that the study was conducted without any commercial or financial relationships that might be considered as a potential conflict of interest.

Ethical approval The studies involved human participants were reviewed and supported by the Ethical Committee of Shanghai Pulmonary Hospital (K18-089-1).

Consent to participate All 26 participants provided their written informed consent to participate in this study.

References

Addeo A, Obeid M, Friedlaender A (2020) COVID-19 and lung cancer: risks, mechanisms and treatment interactions. J Immunother Cancer. https://doi.org/10.1136/jitc-2020-000892

Binnewies M, Roberts EW, Kersten K, Chan V, Fearon DF, Merad M, Coussens LM, Gabrilovich DI, Ostrand-Rosenberg S, Hedrick CC, Vonderheide RH, Pittet MJ, Jain RK, Zou W, Howcroft TK, Woodhouse EC, Weinberg RA, Krummel MF (2018) Understanding the tumor immune microenvironment (TIME) for

effective therapy. Nat Med 24(5):541–550. https://doi.org/10.1038/s41591-018-0014-x
Chai P, Yu J, Ge S, Jia R, Fan X (2020) Genetic alteration, RNA expression, and DNA methylation profiling of coronavirus disease 2019 (COVID-19) receptor ACE2 in malignancies: a pan-cancer analysis. J Hematol Oncol 13(1):43. https://doi.org/10.1186/s13045-020-00883-5
Chang JT, Lee YM, Huang RS (2015) The impact of the cancer genome atlas on lung cancer. Transl Res 166(6):568–585. https://doi.org/10.1016/j.trsl.2015.08.001
Chen F, Zhuang X, Lin L, Yu P, Wang Y, Shi Y, Hu G, Sun Y (2015) New horizons in tumor microenvironment biology: challenges and opportunities. BMC Med 13:45. https://doi.org/10.1186/s12916-015-0278-7
de Sousa VML, Carvalho L (2018) Heterogeneity in lung cancer. Pathobiology 85(1–2):96–107. https://doi.org/10.1159/000487440
Giotopoulou GA, Stathopoulos GT (2020) Effects of inhaled tobacco smoke on the pulmonary tumor microenvironment. Adv Exp Med Biol 1225:53–69. https://doi.org/10.1007/978-3-030-35727-6_4
Herbst RS, Heymach JV, Lippman SM (2008) Lung cancer. N Engl J Med 359(13):1367–1380. https://doi.org/10.1056/NEJMra0802714
Hoffmann M, Kleine-Weber H, Pöhlmann S (2020a) A multibasic cleavage site in the spike protein of SARS-CoV-2 is essential for infection of human lung cells. Mol Cell 78(4):779–84.e5. https://doi.org/10.1016/j.molcel.2020.04.022
Hoffmann M, Kleine-Weber H, Schroeder S, Krüger N, Herrler T, Erichsen S, Schiergens TS, Herrler G, Wu NH, Nitsche A, Müller MA, Drosten C, Pöhlmann S (2020b) SARS-CoV-2 cell entry depends on ACE2 and TMPRSS2 and is blocked by a clinically proven protease inhibitor. Cell 181(2):271–80.e8. https://doi.org/10.1016/j.cell.2020.02.052
Jackson CB, Farzan M, Chen B, Choe H (2022) Mechanisms of SARS-CoV-2 entry into cells. Nat Rev Mol Cell Biol 23(1):3–20. https://doi.org/10.1038/s41580-021-00418-x
Kong Q, Xiang Z, Wu Y, Gu Y, Guo J, Geng F (2020) Analysis of the susceptibility of lung cancer patients to SARS-CoV-2 infection. Mol Cancer 19(1):80. https://doi.org/10.1186/s12943-020-01209-2
Meng B, Abdullahi A, Ferreira I, Goonawardane N, Saito A, Kimura I, Yamasoba D, Gerber PP, Fatihi S, Rathore S, Zepeda SK, Papa G, Kemp SA, Ikeda T, Toyoda M, Tan TS, Kuramochi J, Mitsunaga S, Ueno T, Shirakawa K, Takaori-Kondo A, Brevini T, Mallery DL, Charles OJ, Bowen JE, Joshi A, Walls AC, Jackson L, Martin D, Smith KGC, Bradley J, Briggs JAG, Choi J, Madissoon E, Meyer KB, Mlcochova P, Ceron-Gutierrez L, Doffinger R, Teichmann SA, Fisher AJ, Pizzuto MS, de Marco A, Corti D, Hosmillo M, Lee JH, James LC, Thukral L, Veesler D, Sigal A, Sampaziotis F, Goodfellow IG, Matheson NJ, Sato K, Gupta RK (2022) Altered TMPRSS2 usage by SARS-CoV-2 omicron impacts infectivity and fusogenicity. Nature 603(7902):706–714. https://doi.org/10.1038/s41586-022-04474-x
Onder G, Rezza G, Brusaferro S (2020) Case-fatality rate and characteristics of patients dying in relation to COVID-19 in Italy. JAMA. https://doi.org/10.1001/jama.2020.4683
Ostman A (2012) The tumor microenvironment controls drug sensitivity. Nat Med 18(9):1332–1334. https://doi.org/10.1038/nm.2938
Paces J, Strizova Z, Smrz D, Cerny J (2020) COVID-19 and the immune system. Physiol Res. https://doi.org/10.33549/physiolres.934492
Rogado J, Pangua C, Serrano-Montero G, Obispo B, Marino AM, Pérez-Pérez M, López-Alfonso A, Gullón P, Lara M (2020) Covid-19 and lung cancer: a greater fatality rate? Lung Cancer 146:19–22. https://doi.org/10.1016/j.lungcan.2020.05.034
Rossato M, Russo L, Mazzocut S, Di Vincenzo A, Fioretto P, Vettor R (2020) Current smoking is not associated with COVID-19. Eur Respir J. https://doi.org/10.1183/13993003.01290-2020
Shang J, Wan Y, Luo C, Ye G, Geng Q, Auerbach A, Li F (2020) Cell entry mechanisms of SARS-CoV-2. Proc Natl Acad Sci U S A 117(21):11727–11734. https://doi.org/10.1073/pnas.2003138117
Smith JC, Sausville EL, Girish V, Yuan ML, Vasudevan A, John KM, Sheltzer JM (2020) Cigarette smoke exposure and inflammatory signaling increase the expression of the SARS-CoV-2 receptor ACE2 in the respiratory tract. Dev Cell 53(5):514–29.e3. https://doi.org/10.1016/j.devcel.2020.05.012
Williamson EJ, Walker AJ, Bhaskaran K, Bacon S, Bates C, Morton CE, Curtis HJ, Mehrkar A, Evans D, Inglesby P, Cockburn J, McDonald HI, MacKenna B, Tomlinson L, Douglas IJ, Rentsch CT, Mathur R, Wong AYS, Grieve R, Harrison D, Forbes H, Schultze A, Croker R, Parry J, Hester F, Harper S, Perera R, Evans SJW, Smeeth L, Goldacre B (2020) Factors associated with COVID-19-related death using OpenSAFELY. Nature 584(7821):430–436. https://doi.org/10.1038/s41586-020-2521-4
Wu T, Dai Y (2017) Tumor microenvironment and therapeutic response. Cancer Lett 387:61–68. https://doi.org/10.1016/j.canlet.2016.01.043
Xu B, Chen Q, Yue C, Lan L, Jiang J, Shen Y, Lu B (2018) Prognostic value of IL-6R mRNA in lung adenocarcinoma and squamous cell carcinoma. Oncol Lett 16(3):2935–2948. https://doi.org/10.3892/ol.2018.9044
Yang D, Liu Y, Bai C, Wang X, Powell CA (2020) Epidemiology of lung cancer and lung cancer screening programs in China and the United States. Cancer Lett 468:82–87. https://doi.org/10.1016/j.canlet.2019.10.009
Yu J, Ouyang W, Chua MLK, Xie C (2020) SARS-CoV-2 transmission in patients with cancer at a tertiary care hospital in Wuhan, China. JAMA Oncol. https://doi.org/10.1001/jamaoncol.2020.0980
Zhang X, Peng L, Luo Y, Zhang S, Pu Y, Chen Y, Guo W, Yao J, Shao M, Fan W, Cui Q, Xi Y, Sun Y, Niu X, Zhao X, Chen L, Wang Y, Liu Y, Yang X, Wang C, Zhong C, Tan W, Wang J, Wu C, Lin D (2021) Dissecting esophageal squamous-cell carcinoma ecosystem by single-cell transcriptomic analysis. Nat Commun 12(1):5291. https://doi.org/10.1038/s41467-021-25539-x
Zhou F, Yu T, Du R, Fan G, Liu Y, Liu Z, Xiang J, Wang Y, Song B, Gu X, Guan L, Wei Y, Li H, Wu X, Xu J, Tu S, Zhang Y, Chen H, Cao B (2020) Clinical course and risk factors for mortality of adult inpatients with COVID-19 in Wuhan, China: a retrospective cohort study. Lancet 395(10229):1054–1062. https://doi.org/10.1016/s0140-6736(20)30566-3
Zou X, Chen K, Zou J, Han P, Hao J, Han Z (2020) Single-cell RNA-seq data analysis on the receptor ACE2 expression reveals the potential risk of different human organs vulnerable to 2019-nCoV infection. Front Med 14(2):185–192. https://doi.org/10.1007/s11684-020-0754-0